Biochimica et Biophysica Acta 1858 (2016) 2050–2059

Contents lists available at ScienceDirect

Biochimica et Biophysica Acta

journal homepage: www.elsevier.com/locate/bbamem

Free fatty acids chain length distribution affects the permeability of skin lipid model membranes

Masayuki Uchiyama [a,c,1], Masashi Oguri [b,c,1], Enamul H. Mojumdar [b], Gert S. Gooris [b], Joke A. Bouwstra [b,*]

[a] Tokyo Research Laboratories, Kao Corporation, Bunka, Sumida-ku, Tokyo 131-8501, Japan
[b] Tochigi Research Laboratories, Kao Corporation, Ichikai, Haga, Tochigi 321-3497, Japan
[c] Leiden/Amsterdam Center for Drug Research, Department of Drug Delivery Technology, Leiden University, 2300 RA Leiden, The Netherlands

ARTICLE INFO

Article history:
Received 14 December 2015
Received in revised form 19 May 2016
Accepted 2 June 2016
Available online 7 June 2016

Keywords:
Stratum corneum
Skin
Lipid organization
Permeation
Barrier function

ABSTRACT

The lipid matrix in the stratum corneum (SC) plays an important role in the barrier function of the skin. The main lipid classes in this lipid matrix are ceramides (CERs), cholesterol (CHOL) and free fatty acids (FFAs). The aim of this study was to determine whether a variation in CER subclass composition and chain length distribution of FFAs affect the permeability of this matrix. To examine this, we make use of lipid model membranes, referred to as stratum corneum substitute (SCS). We prepared SCS containing i) single CER subclass with either a single FFA or a mixture of FFAs and CHOL, or ii) a mixture of various CER subclasses with either a single FFA or a mixture of FFAs and CHOL. In vitro permeation studies were performed using ethyl-*p*-aminobenzoic acid (E-PABA) as a model drug. The flux of E-PABA across the SCS containing the mixture of FFAs was higher than that across the SCS containing a single FA with a chain length of 24 C atoms (FA C24), while the E-PABA flux was not effected by the CER composition. To select the underlying factors for the changes in permeability, the SCSs were examined by Fourier transform infrared spectroscopy (FTIR) and Small angle X-ray scattering (SAXS). All lipid models demonstrated a similar phase behavior. However, when focusing on the conformational ordering of the individual FFA chains, the shorter chain FFA (with a chain length of 16, 18 or 20 C atoms forming only 11 m/m% of the total FFA level) had a higher conformational disordering, while the conformational ordering of the chains of the CER and FA C24 and FA C22 hardly did not change irrespective of the composition of the SCS. In conclusion, the conformational mobility of the short chain FFAs present only at low levels in the model SC lipid membranes has a great impact on the permeability of E-PABA.

1. Introduction

The outermost layer of the skin is the stratum corneum (SC), which consists of dead cells (the corneocytes) surrounded by a lipid matrix (intercellular lipid). This matrix is mainly composed of ceramides (CERs), cholesterol (CHOL) and free fatty acids (FFAs) [1,2]. The lipid matrix is considered to provide a diffusion pathway across the SC for foreign substances that are applied onto the skin [3]. The lipids are organized in two coexisting lamellar phases: the short periodicity phase (SPP) with a periodicity of approximately 6 nm, and the long periodicity phase (LPP) with a periodicity of approximately 13 nm [4,5]. Considering the lateral packing within the lipid lamellar at the human skin surface temperature (approximately 32 °C), the lipids are organized mainly in an orthorhombic packing, although a low level of lipids forms also a hexagonal or even a liquid crystalline packing. As an important penetration pathway is along the lipid matrix, the lipid organization is considered to play a crucial role in the skin barrier function [6–8]. As far as the fatty acid composition in human SC is concerned, a wide distribution of FFA chain lengths has been observed. The most abundant chain lengths of the FFA mixture are 22, 24 and 26 carbon atoms [9]. In addition an increasing number of CER subclasses has been identified [10–12]. The CER subclasses differ from each other by the head group architecture and acyl chain length distribution.

Several groups study the fundamental interactions between single CER, CHOL and FFA [13–18]. However, when mimicking the SC lipid composition and organization more complex mixtures are required. These complex compositions has been used in SC lipid model membranes to examine the relationship between the SC lipid barrier function, lipid organization and lipid composition [19]. Using these lipid membranes, referred to as stratum corneum substitutes (SCS), it was reported that a reduction in FFA mean chain length results in a change in the long range ordering with a predominant hexagonal packing at 32 °C and an increased permeability [20]. In these mixtures, there was a substantial increase in the level of FFA with a chain length of 16 and 18

* Corresponding author at: Department of Drug Delivery Technology, Leiden Academic Center for Drug Research, Einsteinweg 55, 2333 CC Leiden, The Netherlands.
E-mail address: bouwstra@chem.leidenuniv.nl (J.A. Bouwstra).
[1] Denotes shared first authorship.

http://dx.doi.org/10.1016/j.bbamem.2016.06.001
0005-2736/

carbon atoms, and a reduction in the level with 24 carbon atoms mimicking the FFA composition in cultured skin. In another study, the effect of acyl chain length of CER NS (a non-hydroxy fatty acid (N) linked to a sphingoid base (S)) on the permeability has been reported [21] and it was shown that longer acyl chains in the CER NS subclass also present in the SC are essential for maintaining the barrier in these lipid membranes. However, in these report permeability changes are only observed with very short chains. Finally, it was also observed that SCS prepared with CERs isolated from pig skin resulted in a much higher permeability of the SCS than a similar CER composition composed of synthetic CERs without a chain length variation [22].

The present study focuses on whether a variation in chain length distribution of fatty acids or a variation in the CER subclass composition affects the permeability of the SCS. This is of interest as both, a wider distribution in chain lengths and a change in CER subclasses composition both occur in inflammatory skin diseases, such as atopic dermatitis, psoriasis and Netherton syndrome patients [23–25]. To examine the permeability of the SCSs, in vitro permeation studies were carried out using ethyl-*p*-aminobenzoic acid (E-PABA). To provide information on the underlying changes in the lipid organization responsible for these changes, Fourier transform infrared spectroscopy (FTIR) was used to examine the lateral packing and conformational ordering. To provide information on the lamellar phases, X-ray scattering (SAXS) studies were performed.

Our studies show that the fatty acid chain length distribution affects the permeability dramatically, while the head group variation of the CER subclasses has no effect.

2. Materials and methods

2.1. Chemicals

CERs: The nomenclature of the abbreviations of the CERs used in this study are as follows [26]. Ceramides are composed of either a sphingosine (S) or a phytosphingosine (P) base having a chain length of 18 carbon atoms. Concerning the acyl chains linked to the sphingoid base, these are either non-hydroxy acyl chain (N) with either a chain length of 24 carbon atoms (C24) or with a chain length of 16 atoms (C16) or an α-hydroxy acyl chain with a chain length of C24. The synthetic CERs used in this study are CER NS, CER NP, CER NP(C16), CER AS and CER AP. CER NP(C16) is an exception with a shorter chain length. These CERs were generously provided by Evonik (Essen, Germany).

The perdeuterated FFA (referred to as DFFA) with chain lengths of C18:0 and C20:0 were purchased from Cambridge Isotope Laboratories (Andover, Massachusetts). The DFFA with chain lengths of C16:0 and C22:0 were obtained from Larodan (Malmö, Sweden). The DFFA with a chain length of C24:0 was obtained from Arc Laboratories B.V. (Apeldoorn, The Netherlands). Cholesterol, ethyl-*p*-aminobenzoic acid (referred to as E-PABA) and acetate buffer salts were provided by Sigma-Aldrich Chemie GmbH (Schnelldorf, Germany). All organic solvents were manufactured by Labscan Ltd. (Dublin, Ireland). All chemicals used were of analytical grade. The chemical structure is depicted in Fig. 1. The CERs were kindly provided by Evonik (Essen, Germany).

2.2. Composition of the lipid mixtures

For the preparation of the SCS, CERs, CHOL, and FFAs were used in an equimolar ratio. The CER subclasses were mixed in a molar ratio of 60:19:5:11:6 for CER NS: CER NP: CER AS: CER NP(C16): CER AP. This ratio resembles very closely the CER composition in pig SC, except that acyl CERs are not present. This specific mixture is referred to as CER_{mix}. The FFA mixture was composed of fatty acids with chain lengths of C16:0, C18:0, C20:0, C22:0 and C24:0 in a molar ratio of 1.8:4.0:7.6:47.8:38.9 respectively, mimicking the composition in SC [27]. In total, four different model lipid mixtures were selected: (CER_{mix}/CHOL/FFAs), (CER NS/CHOL/FFAs), (CER_{mix}/CHOL/FA24) and (CER NS/CHOL/FA24) mixtures were prepared. The FA24 is a single FFA with a chain length of 24 C atoms. To prepare samples for FTIR and SAXD the lipids were dissolved in chloroform/methanol (2:1, v/v) at a lipid concentration of 7.5 mg/ml. For permeability studies the appropriate amount of individual lipids was dissolved in hexane/ethanol (2:1, v/v) at a lipid concentration of 4.5 mg/ml.

2.3. Preparation of SCS for diffusion and X-ray diffraction studies

A 200 μl solution of lipids (4.5 mg/ml) in hexane/ethanol was sprayed in an area of 64 mm^2 on a porous filter (Whatman Nuclepore Track-Etch Membrane, pore size 0.05 μm). The sample was equilibrated for 10 min at around 80 °C close to the melting temperature of the mixture under a stream of dry nitrogen. Then the sample was slowly cooled to room temperature in about 30 min. This heating/cooling cycle was repeated once more. In vitro permeation studies were performed using Permegear inline diffusion cells (Bethlehem, PA, USA) with a diffusion area of 0.28 cm^2. The porous filters with lipid membrane were mounted in the diffusion cells and were hydrated underneath with a acceptor solution for a few hours in phosphate-buffered saline pH 7.4 (PBS: NaCl, Na_2HPO_4,· $12H_2O$ KH_2PO_4 and KCl in MilliQ water with a concentration of 8.00, 2.86, 0.20 and 0.19 g/l, respectively). The donor compartment was filled with 1.4 ml of E-PABA solution in acetate buffer pH 5.0 at a 650 μg/ml concentration. The acceptor phase consisted of PBS (pH 7.4), which was perfused at a flow rate of about 2 ml/h. The acceptor phase was stirred with a magnetic stirrer. The volume of the fractions collected per hour were determined by weighing. All experiments were carried out under occlusive conditions since the opening side of the donor compartment was closed with adhesive tape. To evaluate the permeability of E-PABA under the in vivo conditions, the temperature of the model lipid membranes was maintained at 32 °C during the total length of the experiment by using a thermo-stated water bath. Fractions were collected during a period of 20 h. In addition, the permeability of SCS prepared from CER NS/CHOL/FFAs and CER NS/CHOL/FA24 was also investigated at 24 °C and 36 °C. The permeation studies of all four samples at various temperatures were replicated at least four times.

2.4. FTIR studies

The 200 μl of lipid mixtures dissolved in chloroform/methanol (7.5 mg/ml) were sprayed in an area of 100 mm^2 on an AgBr window by using a Linomat IV (CAMAG, Muttenz, Switzerland). The sample was heated to 90 °C with a rate of 0.5 °C/min and equilibrated for 10 min at 90 °C under a stream of dry air. Then, the sample was cooled slowly to 20 °C with a rate of 1.0 °C. This heating/cooling cycle was repeated once more. Subsequently, the lipid membrane was covered with 25 μl of deuterated acetate buffer pH 5.0 (50 mM) and stored at 37 °C for 10 h to hydrate the sample. To obtain information on the lateral packing and conformational ordering of the lipids, all spectra were acquired on a Varian 670 FT-IR spectrometer (Varian Medical Systems, Inc.) equipped with a broad-band mercury cadmium telluride detector (MCT). This detector is cooled by liquid nitrogen. The sample was under continuous dry air purge starting 30 min before the data acquisition. The spectra were collected in transmission mode, as a co-addition of 256 scans at 1 cm^{-1} resolution during 4 min. In order to detect phase transitions, the sample temperature was increased at a heating rate of 0.25 °C/min resulting in a 1 °C temperature rise per recorded spectrum. The spectra were collected between 0 °C and 90 °C and deconvoluted using a half-width of 4 cm^{-1} and an enhancement factor of 1.7. The software used was Varian resolution pro from Varian. The scanning range was 600–4000 cm^{-1} and the resolution was 1 cm^{-1}. All four samples for investigating the lipid organization were measured at least twice.

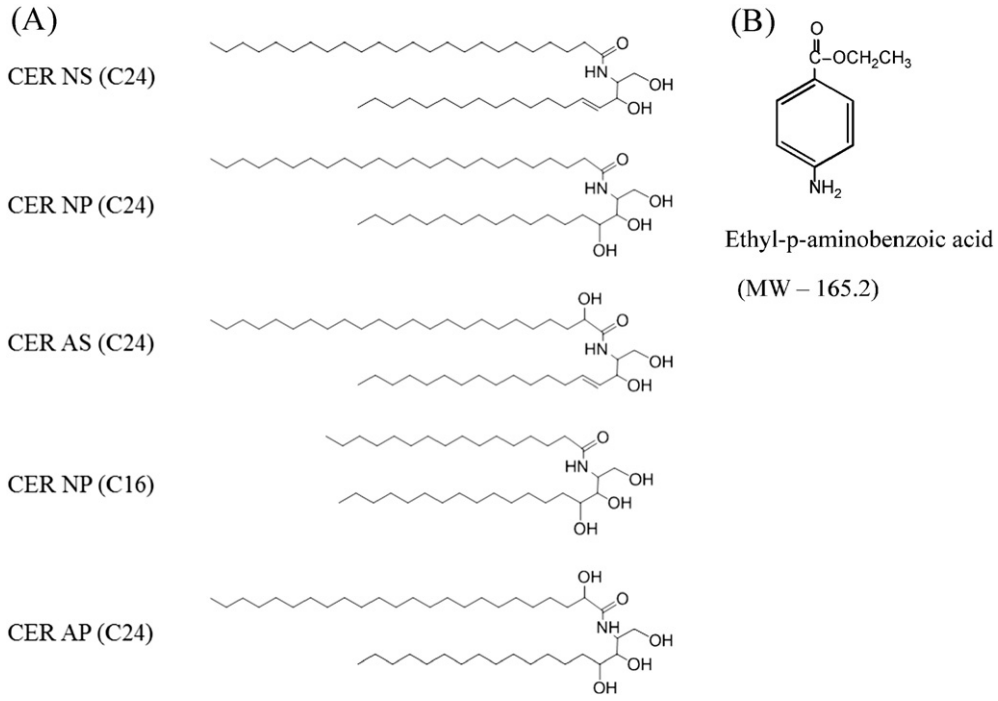

Fig. 1. (A) The structure of the CER subclasses. The CERs consists of an acyl chain attached to a sphingoid base through an amide linkage. (B) The structure of the ethyl-*p*-aminobenzoic acid is also depicted.

2.5. Determining the midpoint temperature of the phase transition in FTIR spectrum

The frequency of the $\nu_s CH_2$ indicates the conformational ordering of the lipid chains: a higher wavenumber indicates an increment disordering of the lipid chains. In case of plotting the peak top of the $\nu_s CH_2$ vibration as a function of temperature, two lipid phase transitions can be detected in the lipid mixtures, the orthorhombic (OR)–hexagonal (HEX) phase transition and the hexagonal–liquid (LIQ) phase transition. In this study, the midpoint temperature of the OR–HEX phase transition was determined by fitting with three linear functions to use a four-pair-parameter function of the temperature and frequency, respectively [28].

2.6. The curve fitting of FTIR spectral

The details of scissoring curve fitting was described earlier [29]. Briefly, the scissoring contours in the FTIR spectra at 32 °C of the lipid mixtures were fitted using the following Lorentz function for the peaks based on the orthorhombic packing and gauss function for the peak based on the hexagonal packing:

$$\text{Lorentz function}: y = \left({}^{2A}\!/_{\pi}\right) \cdot \left\{ {}^{w}\!/_{4(x-x_0)^2} + w^2 \right\}$$

$$\text{Gauss function}: y = \left({}^{A}\!/_{w\sqrt{\pi}/_2} \right) \cdot e^{-2\frac{(x-x_0)^2}{w^2}}$$

Here the peak area is represented by A, w is the full width at its half maximum and the center of the peak is written by x_0. The baseline correction was determined between 1455 and 1480 cm^{-1} region and settled as a background (using the software OriginPro 8.5 from the OriginLab Corporation, Northampton, USA). The fitting procedure (using Python script software) minimizes the deviations between the theoretical and experimental spectra by using the minimization algorithm based on the nonlinear least square method.

2.7. SAXD studies for the analysis of lamellar organization

SAXD was used to determine in which lamellar phases the lipids assembled in the SCS. The scattering intensity I was measured as function of the scattering vector q (in reciprocal nm). The latter is defined as $q = (4\pi\sin\theta)/\lambda$, in which θ is the scattering angle and λ is the wavelength. From the positions of the peaks (q_n), the periodicity of a lamellar phase was calculated using the equation $d = 2n\pi/q_n$, in which n is the order of the diffraction peak and q_n its position at the q axis. For a lamellar phase all peaks are at the same interpeak distance. Data collection was performed at the European Synchrotron Radiation Facility (ESRF, Grenoble) using station BM26B. The sample to detector distance was 2 m and the X-ray wavelength was 0.1033 nm. Diffraction data were collected on a PILATUS 1M detector with 1043 × 981 pixels of 172 μm spatial resolution. The calibration of this detector was carried out using silver behenate ($d = 5.838$ nm for AgBeh). One-dimensional intensity profiles were obtained as described previously [29].

2.8. HPLC analysis

The fractions were analyzed using a reverse-phase high performance liquid chromatographic (HPLC) assay. The HPLC system consisted of a Separations high precision pump (Model 300, H.I. Ambacht, The Netherlands) equipped with a Gilson 234 auto injector and a Spectra SYSTEM UV2000 detector (Thermo Separation Products Inc., California, USA). A reversed phase C18 column (Alltima, C-18, 5 μm, 4.6 × 150 mm) was used as stationary phase. The mobile phase for E-PABA consisted of acetonitrile and water in a ratio of 65:35. The flow rate and the detection wavelength were set to 1.0 ml/min and 286 nm, respectively. A series of standards was run with each series of samples.

3. Results

3.1. The FFA chain length variation affects the lipid barrier function

In Fig. 2(A) the average fluxes of E-PABA obtained at 32 °C are provided. There is no difference between the E-PABA fluxes across SCS prepared using either CER NS or CER_{mix}. The average flux values between 5 h and 20 h of the CER_{mix}/CHOL/FFAs and CER NS/CHOL/FFAs, are 30.9 ± 7.6 μg/cm²/h and 30.2 ± 4.6 μg/cm²/h, respectively. However, when comparing the results obtained with SCS prepared with CER_{mix}/CHOL/FFAs or CER NS/CHOL/FFAs with those prepared with CER_{mix}/CHOL/FA24 or CER NS/CHOL/FA24, the fluxes of the latter are dramatically lower being only 4.9 ± 1.6 μg/cm²/h and 6.7 ± 1.9 μg/cm²/h, respectively. This demonstrates that at 32 °C, mixtures prepared with FFAs results in much higher fluxes than mixtures prepared with FA24. As we questioned whether this strong effect of FFA chain length

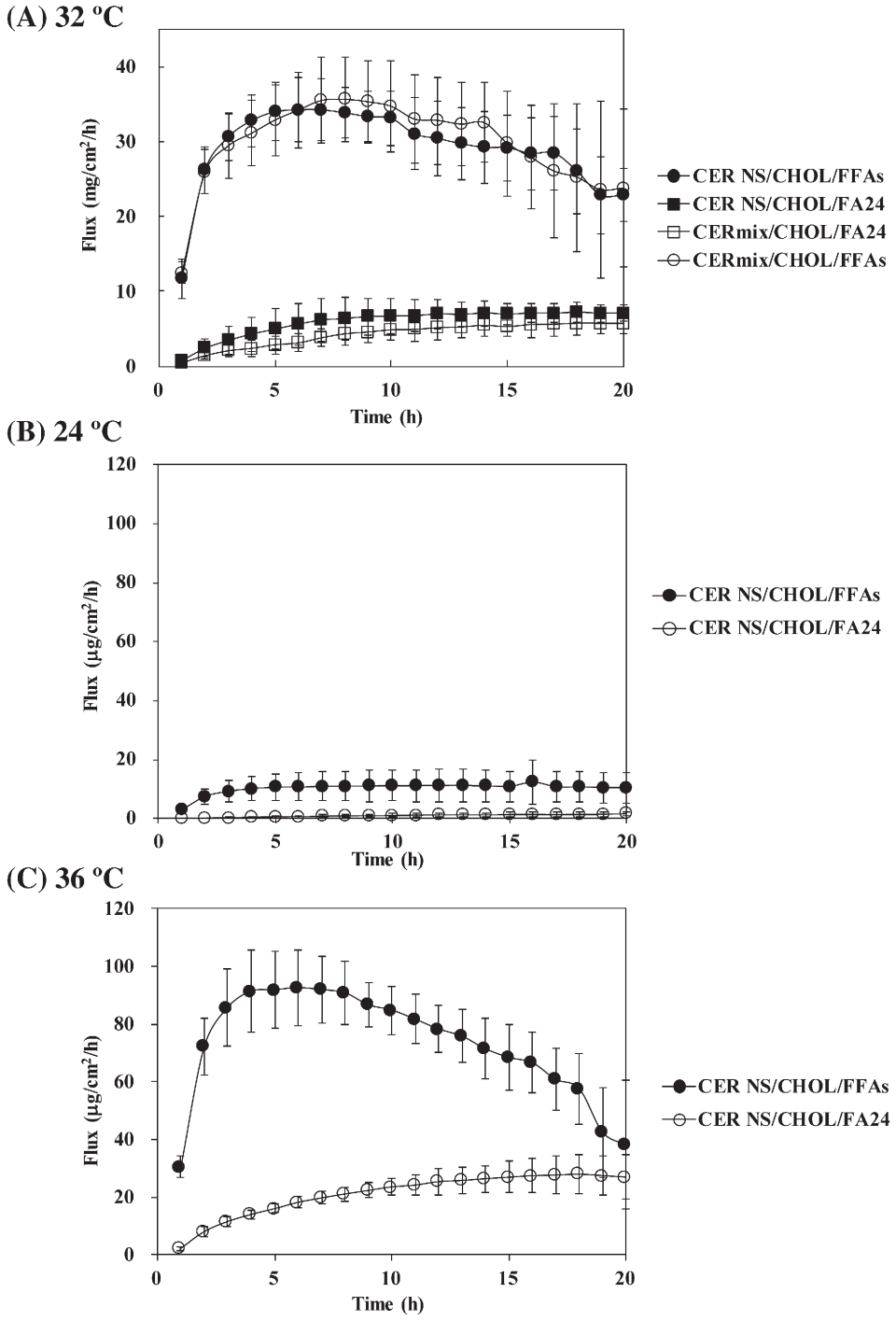

Fig. 2. Fluxes E-PABA across SCS at different composition and temperature (A) fluxes across SCS performed at 32 °C. The compositions of the membranes are CER_{mix}/CHOL/FFAs (open circle), CER NS/CHOL/FFAs (filled circle), CER NS/CHOL/FA24 (filled square) and CER_{mix}/CHOL/FA24 (open square). (B) Fluxes across SCS obtained at 24 °C through SCS composed of CER NS/CHOL/FFAs (filled circle) and CER NS/CHOL/FA24 (open circle). (C) Fluxes across SCS obtained at 36 °C through SCS composed of CER NS/CHOL/FFAs (filled circle) and CER NS/CHOL/FA24 (open circle).

distribution also exists at other temperatures, flux studies were also performed at 24 and 36 °C.

3.2. The flux of E-PABA across the lipid membranes at different temperatures

Additional permeation studies were carried out at 24 °C and 36 °C using SCS prepared with a mixture of either CER NS/CHOL/FFAs or CER NS/CHOL/FA24. The fluxes are provided in Fig. 2(B) and (C) and demonstrate an increase in E-PABA flux when increasing the temperature and at each temperature the flux values of the CER NS/CHOL/FFAs are significantly higher than those obtained using SCS prepared of CER NS/CHOL/FA24. The average flux values at 24 °C for the SCS prepared with CER NS/CHOL/FFAs or CER NS/CHOL/FA24 are 11.0 ± 4.8 μg/cm^2/h and 1.2 ± 0.7 μg/cm^2/h. At 36 °C the flux of E-PABA through SCS prepared with CER NS/CHOL/FA24 is 24.2 ± 5.5 μg/cm^2/h. The SCS prepared with CER NS/CHOL/FFAs did not results in steady state fluxes as after around 7 h the flux starts to decrease most likely due to a depletion of the donor phase.

3.3. Lamellar organization in SC lipid models

As striking differences in the E-PABA flux were observed when replacing FFAs by FA24 compared to replacing CER$_{mix}$ by CER NS, it was decided to study the lipid organization. SAXD provide information about formation of the lamellar phases and their periodicities in the lipid mixtures. The diffraction profiles of the mixtures varying in composition are provided in Fig. 3. Each diffraction pattern reveals the presence of four reflections at about q = 1.17, 1.84, 2.34 and 3.51 nm^{-1}. Three reflections correspond to the 1st, 2nd and 3rd-order diffraction peaks of a SPP with a periodicity of 5.4 nm. The peak at q = 1.84 nm^{-1} indicates the presence of phase separated crystalline CHOL. The lamellar organization as determined with SAXS is very similar for all compositions. In addition, no significant difference is observed in the diffraction profiles of the various compositions between 24 °C and 36 °C (data not shown).

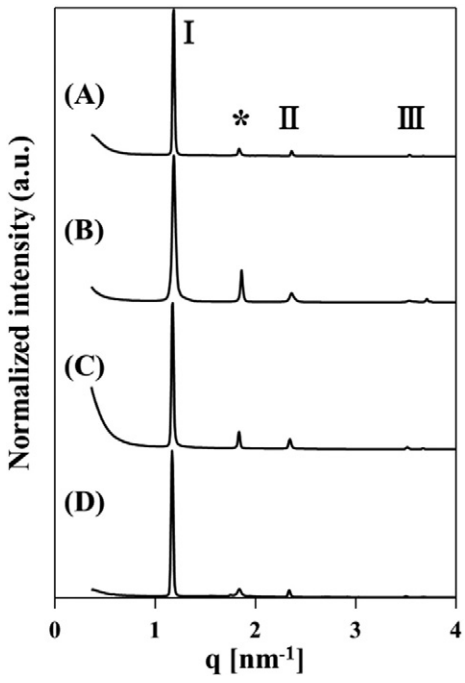

Fig. 3. SAXD patterns of lipid mixtures. (A) CER$_{mix}$/CHOL/FFAs, (B) CER NS/CHOL/FFAs, (C) CER$_{mix}$/CHOL/FA24 and (D) CER NS/CHOL/FA24. The reflections of the SPP are indicated by Roman numbers I, II and III. A diffraction peak from crystalline CHOL is indicated by asterisk.

3.4. Thermal behavior of the lateral packing of various SC lipid models

The FTIR scissoring vibrations provide information about the lateral packing [30–32]. The δCH$_2$ (1462–1473 cm^{-1}) vibrations at 32 °C are shown in Fig. 4. The spectrum reveals a weak doublet in δCH$_2$ vibration frequencies at around 1463 cm^{-1} and 1473 cm^{-1}. This splitting is caused by the short-range coupling of the adjacent lipid tails, indicating the presence of an orthorhombic lateral packing. A peak at around 1468 cm^{-1} indicates the presence of a hexagonal lateral packing. A gradual increase in temperature results in a disappearance of the splitting.

At 32 °C, the spectra of the CER$_{mix}$/CHOL/FFAs and CER NS/CHOL/FFAs show primarily a single peak at about 1467.7 cm^{-1}, which suggests that the lipids mainly adopt a hexagonal phase [30]. The spectra of the CER$_{mix}$/CHOL/FA24 and CER NS/CHOL/FA24 show a broad peak with a shoulder at about 1472 cm^{-1}. This suggests the formation of hexagonal phase with a small fraction of lipids adapting an orthorhombic phase [30].

When focusing on the δCH$_2$ vibrations at 24 °C, all samples show a clear splitting in the contours demonstrating that a part of the lipids assemble in an orthorhombic phase, while the δCH$_2$ vibration at 36 °C, only a single peak is observed. This demonstrates that lipids adopt a hexagonal phase at this temperature (data not shown). This is in line with the results of the stretching vibrations as function of temperature (see Fig. 7(A) and (B)).

3.5. Lorentz and Gauss fitting of the scissoring vibration

In order to examine the contribution of the lipids forming an orthorhombic and those forming a hexagonal lateral packing in the lipid mixtures quantitatively, the scissoring frequencies in the spectra at 32 °C were fitted with a Lorentz (orthorhombic) or Gauss (hexagonal) function. Fig. 5 displays the original and the fitted spectra with their individual curves. The fitting of the original spectra results in COD value close to 1 which indicates an excellent peak fitting. During the fittings the positions and widths were not fixed, but varied. The area of each individual peak contributed to the overall Lorentz and Gauss peak was calculated (See supplement Table S1). For calculating the orthorhombic peak area, the total area of component 1 and 3 was summed, while the area of component 2 represents the hexagonal peak area.

The ratio between the surface area of the δCH$_2$ contour due to lipids assembling in an orthorhombic packing compared to that assembling in a hexagonal packing is provide in Fig. 6. At 32 °C lipid mixtures containing FA24 shows a higher level of lipids adopting the orthorhombic packing than in lipid mixtures containing FFAs.

3.6. Thermal behavior of CH_2 stretching vibration of SC lipid models

Besides the lamellar phases and the lateral packing, the conformational disordering may also play a role in the barrier properties of the SCSs. The ν_sCH$_2$ frequency provides information about the conformational ordering of the lipid tails in the lipid mixtures. A low (~2848 cm^{-1}) wavenumber of the ν_sCH$_2$ indicates the presence of mainly stretched and ordered lipid chains coinciding with a hexagonal or orthorhombic packing, while a high (~2853 cm^{-1}) CH$_2$ wavenumber indicates a low conformational ordering as is present in a liquid phase [31–35].

The ν_sCH$_2$ vibration of the CER$_{mix}$/CHOL/FFAs, CER NS/CHOL/FFAs, CER$_{mix}$/CHOL/FA24 and CER NS/CHOL/FA24 mixtures in FTIR spectrum is examined as a function of temperature and the peak positions of the ν_sCH$_2$ contours as function of temperature are provided in Fig. 7(A) and (B). Two shifts can be identified for the lipid mixtures. The first shift (between 20 °C and 30 °C) and second strong shift (between 60 °C and 75 °C) suggest the orthorhombic–hexagonal phase change and the order-disorder phase change, respectively [30–32]. At temperatures below 30 °C, the ν_sCH$_2$ vibrations of the lipid mixtures indicate

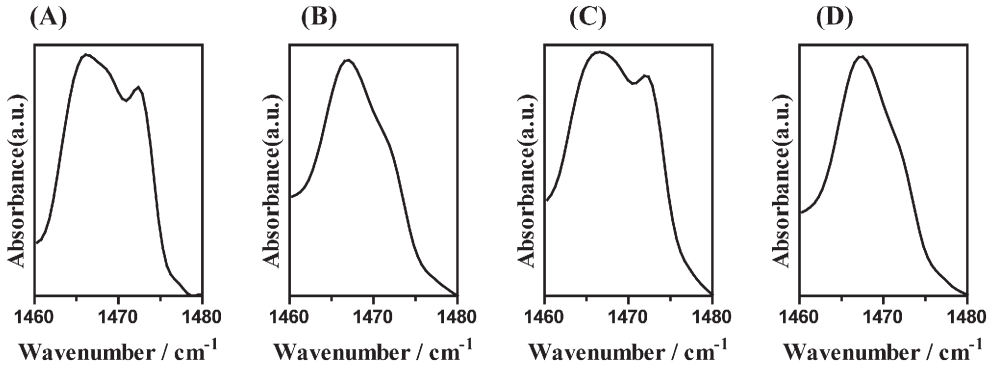

Fig. 4. The δCH_2 vibrations of the various lipid mixtures at 32 °C. (A) CER NS/CHOL/FA24, (B) CER NS/CHOL/FFAs, (C) CER_{mix}/CHOL/FA24 and (D) CER_{mix}/CHOL/FFAs at 32 °C.

highly ordered chains [31]. Only the $\nu_s CH_2$ vibrations in the spectrum of the CER_{mix}/CHOL/FFAs are slightly higher in wavenumber over the whole temperature range, but this shift in wavenumber is not significant.

Besides the values of the $\nu_s CH_2$ vibrations, the phase transition temperatures were also calculated. We decided to use the midpoint temperature of the orthorhombic–hexagonal phase transition. The midpoint temperature of the CER_{mix}/CHOL/FFAs, CER NS/CHOL/FFAs, CER_{mix}/CHOL/FA24 and CER NS/CHOL/FA24 are 23.3 ± 1.3 °C, 26.8 ± 0.7 °C, 29.5 ± 1.1 °C and 30.2 ± 0.3 °C, respectively. When comparing mixtures containing FFAs with those containing FA24, a significant lower midpoint temperature is observed. However, when comparing the mixtures containing CER NS with those containing CER_{mix}, no significant differences are observed in midpoint temperature. The phase transition takes place in the same temperature region at which the diffusion studies were performed. This is the first indication that indeed the $\nu_s CH_2$ vibration of mixtures prepared with FFAs demonstrate some important differences compared to the $\nu_s CH_2$ vibration of mixtures prepared with FA24. Therefore it was decided to go into more details concerning these vibrations.

3.7. The effect of individual FFA on the conformational ordering of SC lipid model system in CD_2 asymmetric stretching vibration

In order to investigate the contribution of each individual FFA in the mixture, protiated FFA are replaced by deuterated counterparts either entirely or partially. The compositions that are used are shown in Table 1. Fig. 8 displays the $\nu_{as} CD_2$ vibrations in the FTIR spectra of the lipid mixtures at three temperatures. The introduction of DFFA allows us to detect whether these specific chains have differences in mobility and whether

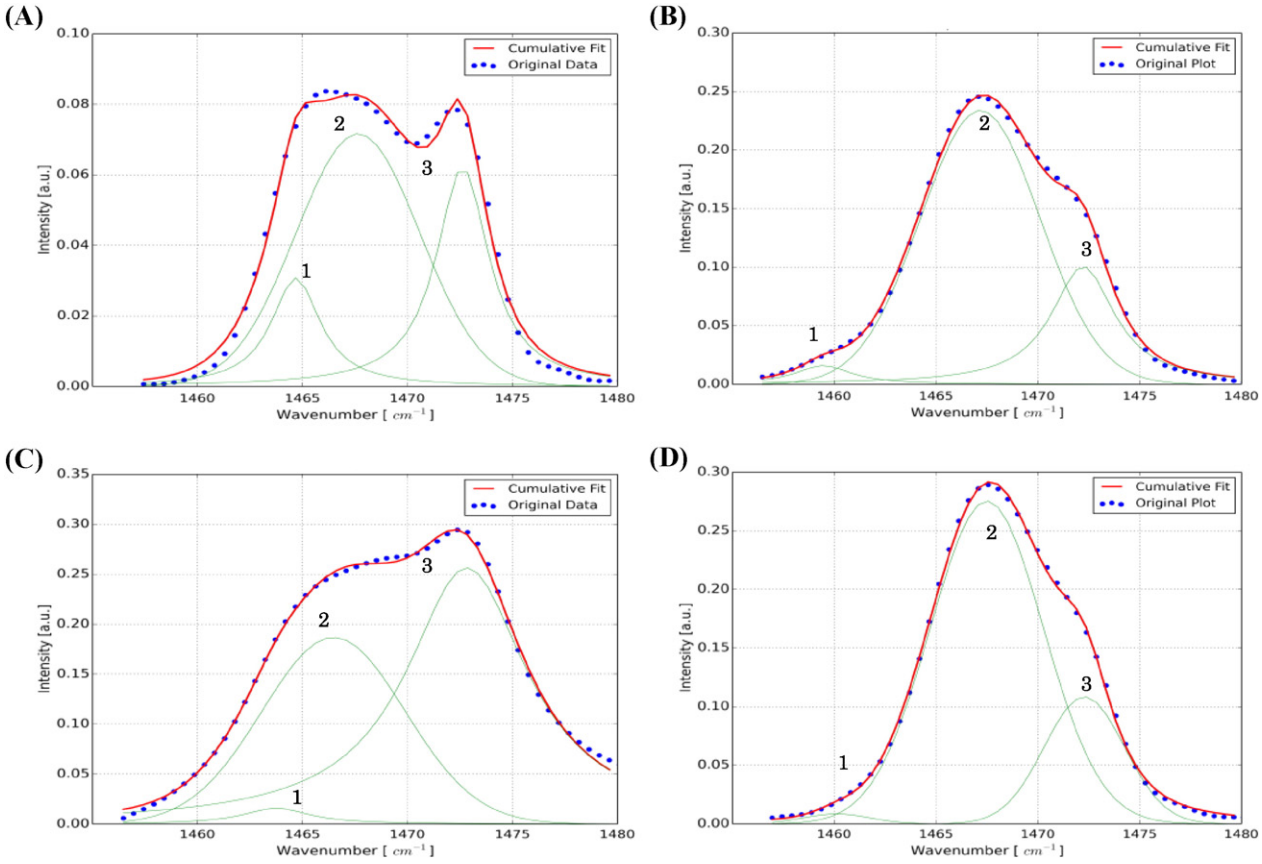

Fig. 5. Lorentz and Gauss fitting of δCH_2 vibration at 32 °C. (A) CER NS/CHOL/FA24, (B) CER NS/CHOL/FFAs, (C) CER_{mix}/CHOL/FA24 and (D) CER_{mix}/CHOL/FFAs dot line is actual curve. Red line is fitted curve. Green line shows each curve representing either δCH_2 due to lipids in a hexagonal phase (curve 2) or due to lipids in the orthorhombic phase (curve 1 and 3).

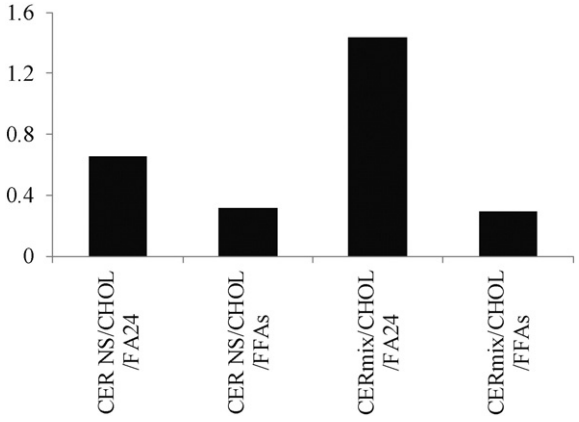

Fig. 6. The ratio between the δCH_2 vibrations of lipids adopting an orthorhombic phase and the δCH_2 vibrations of lipids adopting to a hexagonal packing at 32 °C.

the deuterated chains participate in one lattice with the protiated chains or phase separate. When focusing on the mobility of the selected deuterated chains in the mixtures CER_{mix}/CHOL/$FFAs^{(D16,D18)}$ and CER_{mix}/CHOL/$FFAs^{(D20)}$, a relatively higher $\nu_{as}CD_2$ frequency was observed, indicating that these chains have a higher mobility. When replacing the longer chain FFA by their deuterated counterparts such as CER_{mix}/CHOL/$FFAs^{(D22)}$ and CER_{mix}/CHOL/$FFAs^{(D24)}$, a reduction in the $\nu_{as}CD_2$ wavenumber is detected, illustrating a higher conformational ordering of these chains despite the fact that all FFAs participate in the same lattice (no splitting of scissoring vibrations, see supplement Fig. S1). When replacing FA24 in the FFA mixture by the DFA24 and compare the $\nu_{as}CD_2$ wavenumber in the spectrum of CER_{mix}/CHOL/$FFAs^{(D24)}$ with that in the spectrum of CER_{mix}/CHOL/DFA24, in the latter there is a slightly further reduction in the wavenumber of the $\nu_{as}CD_2$ vibration. Finally, when replacing CER_{mix} by CER NS, no change in the $\nu_{as}CD_2$ is observed, illustrating that the variation in CER composition (chain length as well as head group variation) does not affect the $\nu_{as}CD_2$ vibrations of the deuterated FA chains. Furthermore, the variation in chain ordering of deuterated FFA at the 3 selected temperatures is very small. As the phase transition from orthorhombic to hexagonal lateral packing is not detectable in the thermotropic $\nu_{as}CD_2$ responses, the observed differences in chain order cannot be caused by differences in packing due to an orthorhombic–hexagonal phase transition.

3.8. The interaction of individual FFA on the conformational ordering of SC lipid model system in CH_2 symmetrical vibration

The mixtures, in which differences in molecular mobility were observed in the individual DFFA, were also examined by measuring ν_sCH_2 vibrations of selected lipids. To perform this, mixtures with a lipid composition were prepared as summarized in Table 2. Fig. 9 displays the ν_sCH_2 vibration of all samples measured. When comparing the ν_sCH_2 vibrations in the spectrum of the mixtures CER_{mix}/CHOL/DFFAs, CER_{mix}/CHOL/$DFFAs^{(C16,C18)}$ and CER_{mix}/CHOL/$DFFAs^{(C20)}$, no change in wavenumber is observed, indicating that the low level of FA16/18 or FA20 does not affect the conformational ordering of the CER_{mix}. However, when focusing on the mixtures CER_{mix}/CHOL/$DFFAs^{(C22)}$ and CER_{mix}/CHOL/$DFFAs^{(C24)}$ compared to CER_{mix}/CHOL/DFFAs, a reduction in wavenumber is observed, demonstrating a higher conformational ordering of the FFA with longer chain, that is C22 and C24.

To examine the effect of chain length variation in FFAs on the ν_sCH_2 vibrations attributed to CER_{mix}/CHOL more closely, the ν_sCH_2 vibration of the CER_{mix}/CHOL/$DFFAs^{(C24)}$, CER_{mix}/CHOL/DFFAs and CER_{mix}/CHOL/FA D24 were compared (see Fig. 9). The ν_sCH_2 vibrations in the spectrum of the CER_{mix}/CHOL/FA D24 and CER_{mix}/CHOL/DFFAs are very similar, indicating an almost same mobility of the CER chains irrespective of whether DFA24 or DFFAs have been used. In contrast, the fully protonated CER_{mix}/CHOL/FA24 mixture shows a reduced wavenumber of ν_sCH_2. This demonstrates that the FA24 has a highly ordered acyl chain packing and may be responsible for the reduced integrated ν_sCH_2 vibration. The partially deuterated CER_{mix}/CHOL/$DFFAs^{(C24)}$ shows a higher ν_sCH_2 frequency, demonstrating less ordered conformational packing than the mixture that has been prepared with the single FA24. The ν_sCH_2 frequency of the shorter chain length (C16/C18 and C20) increases confirming the results of the short chain deuterated FA chains. However the ν_sCH_2 frequencies of the shorter chains are difficult to interpret as this can also be due to a change in the interchain coupling (see discussion [36]). These observations have been made at all three selected temperatures.

Table 1
The compositions of the various mixtures used in this study.

Lipid model type	Composition and molar ratio (1.1.1)
CER_{mix}/CHOL/$FFAs^{(D16,D18)}$	CER_{mix}/CHOL/FFAs with FA16 and FA18 replaced by DFA16 and DFA18
CER_{mix}/CHOL/$FFAs^{(D20)}$	CER_{mix}/CHOL/FFAs with FA20 replaced by DFA20
CER_{mix}/CHOL/$FFAs^{(D22)}$	CER_{mix}/CHOL/FFAs with FA22 replaced by DFA22
CER_{mix}/CHOL/$FFAs^{(D24)}$	CER_{mix}/CHOL/FFAs with FA24 replaced by DFA24
CER_{mix}/CHOL/FA D24	CER_{mix}/CHOL/FA24 with FA24 replaced by DFA24
CER NS/CHOL/FA D24	CER NS/CHOL/FA24 with FA24 replaced by DFA24

4. Discussion

In this study, we observed that a variation in chain length distribution of FFAs affects the permeability across the SCS drastically, while a variation in CER head group architecture has no effect. Besides the change in permeability, a small reduction in the transitions temperatures of the

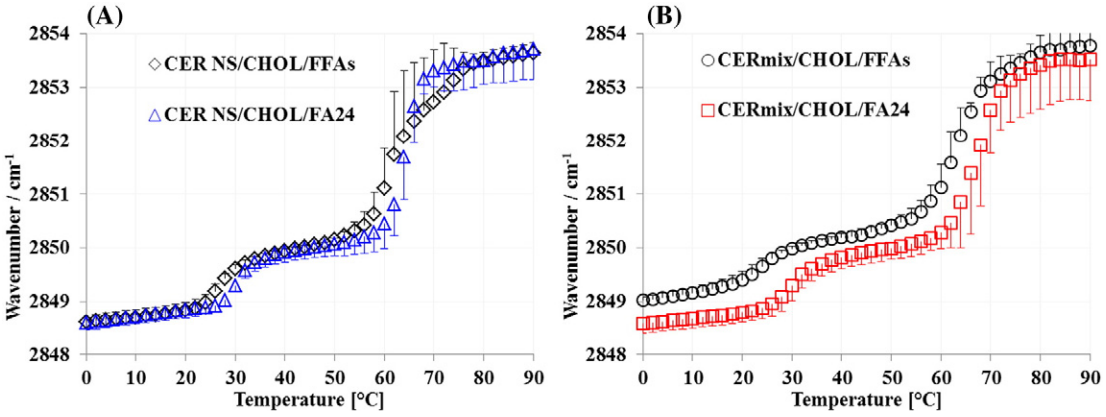

Fig. 7. Thermotropic response of the ν_sCH_2 vibrations. (A) Lipid mixtures prepared with CER NS, (B) lipid mixtures prepared with CER_{mix},

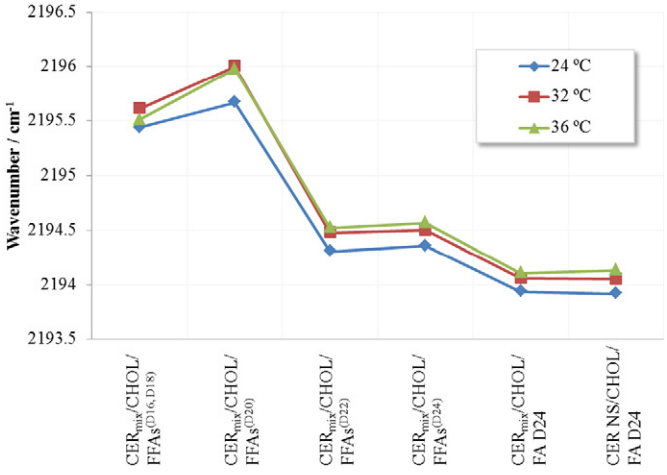

Fig. 8. The $\nu_{as}CD_2$ vibrations of the DFFAs, either DFA16 + 18, DFA20, DFA22, DFA24 all as part of the FFA mixture. Blue line, red line and green line indicate at 24 °C, 32 °C and 36 °C, respectively. The abbreviations of sample are provided in the Table 1.

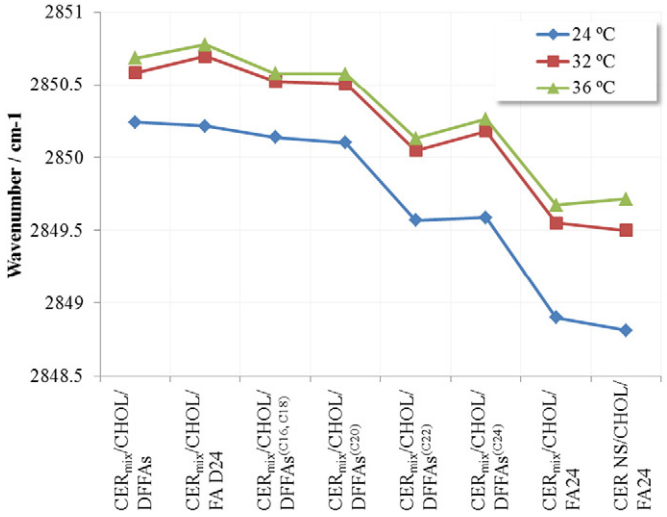

Fig. 9. The ν_sCH_2 vibration in protonated acyl chain. DFFAs were partially replaced by protonated FA. The sample abbreviations are shown in Table 2.

orthorhombic–hexagonal transition was also observed when SCS prepared with the FFA mixture was compared with SCS prepared with the single FA24. This shift in transition to lower temperatures may contribute to a higher permeability at 24 °C and 32 °C. However, at 36 °C, both SCS form a hexagonal lateral packing, but there is still a substantial difference in permeability. Furthermore, using C^{13} NMR these compositions were also measured and no fluid phase was observed (Dat, Sparr et al., unpublished results). Therefore more detailed information to explain the differences in permeability was required. For this reason we studied the lipid mixtures with partially substitution of protiated FFAs by their deuterated counterparts and vice versa. In this way it is possible to examine the stretching vibrations of selected chains. These studies demonstrated that i) low levels of FA16/FA18 or FA20 do not affect the mobility of the CER chains, as the ν_sCH_2 vibrations are very similar in mixtures prepared with DFA24 or DFFAs and ii) the mobility of the shorter chain DFA are high compared to that of the other lipid components in the same lattice, including DFA24: DFA24 introduced in the lipid mixture as part of FFAs or introduced as a single FA resulted in similar $\nu_{as}CD_2$ vibrations. Most probably the $\nu_{as}CD_2$ vibrations with a higher wavenumber of the short chain FA and thus an increased conformational mobility contribute significantly to the increased permeability. Although deuterated chains also increase the ν_sCH_2 vibrations of the protiated chains, the higher $\nu_{as}CD_2$ wavenumbers of the shorter DFA chains being not sensitive for the surrounding chains demonstrates that the mobility of the shorter chains are indeed increased [36,37]. The higher mobility of the shorter chains is an interesting phenomenon that can be extrapolated with some precautions to the observed lipid composition alterations in diseased skin with an impaired barrier function.

Table 2
Various lipid model used in this study. The name of replaced FA is written in superscript on the right.

Lipid model type	Composition and molar ratio (1.1.1)
CER_{mix}/CHOL/DFFAs	CER_{mix}/CHOL/DFFAs with FFAs replaced by deuterated counterparts
CER_{mix}/CHOL/FA D24	CER_{mix}/CHOL/FA24 with FA24 replaced by FA D24
CER_{mix}/CHOL/$DFFAs^{(C16,C18)}$	CER_{mix}/CHOL/DFFAs with DFA16 and DFA18 replaced by FA16 and FA18
CER_{mix}/CHOL/$DFFAs^{(C20)}$	CER_{mix}/CHOL/DFFAs with DFA20 replaced by FA20
CER_{mix}/CHOL/$DFFAs^{(C22)}$	CER_{mix}/CHOL/DFFAs with DFA22 replaced by FA22
CER_{mix}/CHOL/$DFFAs^{(C24)}$	CER_{mix}/CHOL/DFFAs with DFA24 replaced by FA24

4.1. The role of fatty acid profile in the skin barrier of inflammatory skin diseases

In inflammatory skin diseases, such as atopic dermatitis, Netherton syndrome and psoriasis, a reduction in chain length of the lipids has been observed [23–25,38,39]. Both skin diseases suffer from an impaired skin barrier function. In atopic dermatitis patients it has been shown that i) a reduction in lipid chain length correlated excellently with an impaired skin barrier function and ii) the major reduction in fatty acid chain length has been caused by a higher level of shorter FFA, typically increased levels of FA16 and FA18 [23]. Therefore, when extrapolating the findings of the present study and previous studies to that observed in atopic eczema patients, the increased level of short chain FFA may contribute to a higher permeability due to an increase in the stretching vibrations and thus a higher conformational disordering. Not only a shorter chain length has been observed, but also an increase in the level of unsaturated fatty acids in Netherton syndrome patients and in lesional skin of atopic dermatitis patients [23,39]. In previous studies using SCSs an increase in the level of unsaturated FFA reduced the packing density in the lipid organization, thereby increasing the permeability of hydrocortisone across the SCS [40]. This demonstrates that both an increase in short chain FFAs and an increase in the unsaturation level of the FFA may contribute to the impaired skin barrier function.

4.2. The role of CER composition and chain length distribution in the skin barrier of inflammatory skin diseases

In addition, in both atopic dermatitis patients and Netherton syndrome patients, a change in CER subclass composition has also been observed. Our present study, however, shows that changes in the composition of the CER subclasses play a less prominent role in the impaired skin barrier function as the SCS prepared with only CER NS or with a CER_{mix} did not result in a change in permeability. In addition no changes in the conformational ordering were observed and the transition from orthorhombic to hexagonal lateral packing occurred in the same temperature range. Therefore an increase in CER NS and CER AS and a reduction in the level of CER NP as observed in the inflammatory skin diseases are not expected to have a major effect on the skin barrier function.

As far as the ceramide chain length is concerned, only one study has been reported that focused on the CER chain length and it was observed that a chain length reduction increased the permeability drastically with

the short-chain ceramide (acyl chain only 8 C atoms) compared to a longer fatty acid chain ceramide [41]. Theophylline and indomethacin were used as model components. CERs with such very short acyl chains, however, are not observed in diseased skin. In inflammatory skin diseases, a more subtle chain length reduction in the CERs, such as an increased level of CERs with a total chain length of 34 C atoms (sphingoid base and acyl chain) are encountered. This may also contribute to a higher permeability in skin diseases and offers an interesting subject of future research.

In our present study no acylCERs are incorporated in the SCS. These are CERs with a very long ω-hydroxy acyl chains (up to 34 C atoms) and a linoleic acid linked to the acyl chain. The acylCERs play a crucial role in the formation of a lamellar phase with a periodicity of around 13 nm also present in SC. The formation of this phase is also considered to be important for a proper skin barrier function [5,7–9]. Whether a higher conformational disordering of the shorter fatty acids will also exist in SCS that form the LPP remains to be established.

4.3. Increased permeability related to higher conformational disordering

It is remarkable that the increased conformational disordering of such a small fraction of short chain fatty acids results in a drastic increase in the permeability of E-PABA across the crystalline lipid organization of the SCS. Most probably this is not due to a higher solubility of E-PABA in the SCS as the change in lipid composition is minor. It is more likely that there is an increase in the diffusivity of the compound across the SCS [42]. A possible mechanism is an increase in the free volume that would facilitate the transport of the rather small molecules, such as E-PABA across the SCS [43,44]. The increase in free volume may be caused by either the shorter chain (C16, C18 and C20) that fits less perfectly in the molecular arrangement mainly consisting of C22 and C24 FFA chains. The free volume may also be increased by the higher conformational disordering of these shorter FFA chains. Another possibility is a kink formation facilitated by conformational disordering of the chains [45,46]. The kink formation is formed by gauche-trans-gauche conformations and directly associates conformational disordering. This has been described in particularly for transport of water across crystalline membranes. Although E-PABA is much larger in size than water, an accumulation of these kinks may increase gaps for diffusion of E-PABA in the presence or absence of water penetration. However in our study, we could not find evidence for kink formation in the infrared spectra (data not shown).

4.4. Ceramide head group interactions

In the present study, we also investigated whether ceramide head group variation affects permeability using the SCS prepared with either single CER NS or CER_{mix}, respectively. However we did not notice a difference in lamellar organization, conformational ordering and mid transition temperature of orthorhombic to hexagonal phase transition. The amide vibration in the ceramide head group and carbonyl vibration in fatty acids were also examined with the FTIR, but no significant and systematic differences in these vibrations were observed either. Therefore there are no indications that the head group interactions that might be different in CER_{mix} and CER NS contribute to a difference in permeability, although a substantial change in CER subclass composition was used: CER_{mix} is composed of 60% CER NS and 40% other ceramide subclasses.

5. Conclusions

In the present study we examined whether a variation in chain length distribution of free fatty acids or/and a variation in the ceramide subclasses affects the permeability of the model SC lipid membranes. This work demonstrates that a low level of shorter chain FFAs, with a chain length of C16, C18 or C20 affects the flux of E-PABA through SCS, most probably due to a higher conformational disordering of these shorter chain fatty acid. Furthermore, changes in ceramide composition did not affect permeability and conformational disordering demonstrating that a change of CER class composition in particular from CER NP to CER NS is not expected to contribute substantially to an impaired lipid barrier.

Supplementary data to this article can be found online at http://dx.doi.org/10.1016/j.bbamem.2016.06.001.

Conflict of interest

The authors have no conflict of interest directly relevant to the content of this article.

Transparency document

The Transparency document associated with this article can be found in the online version.

Acknowledgement

We would like to thank to the company Evonik (Essen, Germany) for their generous provision of CERs. We also like to thank the personnel in ESRF located at Grenoble, France for their assistance during the X-ray diffraction measurements.

References

[1] P.W. Wertz, M.C. Miethke, S.A. Long, J.S. Strauss, D.T. Downing, The composition of the ceramides from human stratum corneum and from comedones, J. Investig. Dermatol. 84 (1985) 410–412.
[2] K.J. Robson, M.E. Stewart, S. Michelsen, N.D. Lazo, D.T. Downing, 6-Hydroxy-4-sphingenine in human epidermal ceramides, J. Lipid Res. 35 (1994) 2060–2068.
[3] O. Simonetti, A.J. Hoogstraate, W. Bialik, J.A. Kempenaar, A.H. Schrijvers, H.E. Bodde, M. Ponec, Visualization of diffusion pathways across the stratum corneum of native and in-vitro-reconstructed epidermis by confocal laser scanning microscopy, Arch. Dermatol. Res. 287 (1995) 465–473.
[4] J.A. Bouwstra, G.S. Gooris, W. Bras, D.T. Downing, Lipid organization in pig stratum corneum, J. Lipid Res. 36 (1995) 685–695.
[5] J.A. Bouwstra, G.S. Gooris, J.A. van der Spek, W. Bras, Structural investigations of human stratum corneum by small-angle X-ray scattering, J. Investig. Dermatol. 97 (1991) 1005–1012.
[6] S.H. White, D. Mirejovsky, G.I. King, Structure of lamellar lipid domains and corneocyte envelopes of murine stratum corneum. An X-ray diffraction study, Biochemistry 27 (1988) 3725–3732.
[7] J. Bouwstra, G. Gooris, M. Ponec, The lipid organisation of the skin barrier: liquid and crystalline domains coexist in lamellar phases, J. Biol. Phys. 28 (2002) 211–223.
[8] I. Hatta, N. Ohta, K. Inoue, N. Yagi, Coexistence of two domains in intercellular lipid matrix of stratum corneum, Biochim. Biophys. Acta 1758 (2006) 1830–1836.
[9] L. Norlen, I. Nicander, A. Lundsjo, T. Cronholm, B. Forslind, A new HPLC-based method for the quantitative analysis of inner stratum corneum lipids with special reference to the free fatty acid fraction, Arch. Dermatol. Res. 290 (1998) 508–516.
[10] J. van Smeden, L. Hoppel, R. van der Heijden, T. Hankemeier, R.J. Vreeken, J.A. Bouwstra, LC/MS analysis of stratum corneum lipids: ceramide profiling and discovery, J. Lipid Res. 52 (2011) 1211–1221.
[11] R. t'Kindt, L. Jorge, E. Dumont, P. Couturon, F. David, P. Sandra, K. Sandra, Profiling and characterizing skin ceramides using reversed-phase liquid chromatography–quadrupole time-of-flight mass spectrometry, Anal. Chem. 84 (2012) 403–411.
[12] M. Rabionet, K. Gorgas, R. Sandhoff, Ceramide synthesis in the epidermis, Biochim. Biophys. Acta 1841 (2014) 422–434.
[13] M. Lafleur, Phase behavior of model stratum corneum lipid mixtures: an infrared spectroscopy investigation, Can. J. Chem. 76 (1998) 1501–1511.
[14] D.J. Moore, M.E. Rerek, R. Mendelsohn, Role of ceramides 2 and 5 in the structure of the stratum corneum lipid barrier, Int. J. Cosmet. Sci. 21 (1999) 353–368.
[15] V. Velkova, M. Lafleur, Influence of the lipid composition on the organization of skin lipid model mixtures: an infrared spectroscopy investigation, Chem. Phys. Lipids 117 (2002) 63–74.
[16] P. Garidel, B. Folting, I. Schaller, A. Kerth, The microstructure of the stratum corneum lipid barrier: mid-infrared spectroscopic studies of hydrated ceramide:palmitic acid: cholesterol model systems, Biophys. Chem. 150 (2010) 144–156.
[17] A.C. Rowat, N. Kitson, J.L. Thewalt, Interactions of oleic acid and model stratum corneum membranes as seen by ^2H NMR, Int. J. Pharm. 307 (2006) 225–231.
[18] S. Wartewig, R.H. Neubert, Properties of ceramides and their impact on the stratum corneum structure: a review. Part 1: ceramides, Skin Pharmacol. Physiol. 20 (2007) 220–229.
[19] M. de Jager, W. Groenink, R. Bielsa, i. Guivernau, E. Andersson, N. Angelova, M. Ponec, J. Bouwstra, A novel in vitro percutaneous penetration model: evaluation

of barrier properties with p-aminobenzoic acid and two of its derivatives, Pharm. Res. 23 (2006) 951–960.
[20] D. Groen, D.S. Poole, G.S. Gooris, J.A. Bouwstra, Is an orthorhombic lateral packing and a proper lamellar organization important for the skin barrier function? Biochim. Biophys. Acta 1808 (2011) 1529–1537.
[21] B. Janusova, J. Zbytovska, P. Lorenc, H. Vavrysova, K. Palat, A. Hrabalek, K. Vavrova, Effect of ceramide acyl chain length on skin permeability and thermotropic phase behavior of model stratum corneum lipid membranes, Biochim. Biophys. Acta 1811 (2011) 129–137.
[22] E.H. Mojumdar, Z. Kariman, L. van Kerckhove, G.S. Gooris, J.A. Bouwstra, The role of ceramide chain length distribution on the barrier properties of the skin lipid membranes, Biochim. Biophys. Acta 1838 (2014) 2473–2483.
[23] J. van Smeden, M. Janssens, E.C. Kaye, P.J. Caspers, A.P. Lavrijsen, R.J. Vreeken, J.A. Bouwstra, The importance of free fatty acid chain length for the skin barrier function in atopic eczema patients, Exp. Dermatol. 23 (2014) 45–52.
[24] G. Imokawa, A. Abe, K. Jin, Y. Higaki, M. Kawashima, A. Hidano, Decreased level of ceramides in stratum corneum of atopic dermatitis: an etiologic factor in atopic dry skin? J. Investig. Dermatol. 96 (1991) 523–526.
[25] J. Ishikawa, H. Narita, N. Kondo, M. Hotta, Y. Takagi, Y. Masukawa, T. Kitahara, Y. Takema, S. Koyano, S. Yamazaki, A. Hatamochi, Changes in the ceramide profile of atopic dermatitis patients, J. Investig. Dermatol. 130 (2010) 2511–2514.
[26] S. Motta, M. Monti, S. Sesana, R. Caputo, S. Carelli, R. Ghidoni, Ceramide composition of the psoriatic scale, Biochim. Biophys. Acta 1182 (1993) 147–151.
[27] P. Wertz, Epidermal Lipids, in: L.A. Goldsmith (Ed.), Physiology, Biochemistry and Molecular Biology of the Skin, Oxford University Press, Oxford 1991, pp. 205–235.
[28] M. Oguri, G.S. Gooris, K. Bito, J.A. Bouwstra, The effect of the chain length distribution of free fatty acids on the mixing properties of stratum corneum model membranes, Biochim. Biophys. Acta 1838 (2014) 1851–1861.
[29] E.H. Mojumdar, G.S. Gooris, J.A. Bouwstra, Phase behavior of skin lipid mixtures: the effect of cholesterol on lipid organization, Soft Matter 11 (2015) 4326–4336.
[30] G.S. Gooris, J.A. Bouwstra, Infrared spectroscopic study of stratum corneum model membranes prepared from human ceramides, cholesterol, and fatty acids, Biophys. J. 92 (2007) 2785–2795.
[31] D.J. Moore, M.E. Rerek, R. Mendelshon, FTIR spectroscopy studies of the conformational order and phase behavior of ceramides, J. Phys. Chem. B 101 (1997) 8933–8940.
[32] R. Mendelsohn, G.L. Liang, H.L. Strauss, R.G. Snyder, IR spectroscopic determination of gel state miscibility in long-chain phosphatidylcholine mixtures, Biophys. J. 69 (1995) 1987–1998.
[33] M.W. de Jager, G.S. Gooris, M. Ponec, J.A. Bouwstra, Lipid mixtures prepared with well-defined synthetic ceramides closely mimic the unique stratum corneum lipid phase behavior, J. Lipid Res. 46 (2005) 2649–2656.
[34] F. Damien, M. Boncheva, The extent of orthorhombic lipid phases in the stratum corneum determines the barrier efficiency of human skin in vivo, J. Investig. Dermatol. 130 (2010) 611–614.
[35] D. Bommannan, R.O. Potts, R.H. Guy, Examination of stratum corneum barrier function in vivo by infrared spectroscopy, J. Investig. Dermatol. 95 (1990) 403–408.
[36] V.R. Kodati, R. El-Jastimi, M. Lafleur, Contribution of the intermolecular coupling and librotorsional mobility in the methylene stretching modes in the infrared spectra of acyl chains, J. Phys. Chem. 98 (1994) 12191–12197.
[37] X. Chen, S. Kwak, M. Lafleur, M. Bloom, N. Kitson, J. Thewalt, Fatty acids influence "solid" phase formation in models of stratum corneum intercellular membranes, Langmuir 23 (2007) 5548–5556.
[38] C. Tawada, H. Kanoh, M. Nakamura, Y. Mizutani, T. Fujisawa, Y. Banno, M. Seishima, Interferon-gamma decreases ceramides with long-chain fatty acids: possible involvement in atopic dermatitis and psoriasis, J. Investig. Dermatol. 134 (2014) 712–718.
[39] J. van Smeden, M. Janssens, W.A. Boiten, V. van Drongelen, L. Furio, R.J. Vreeken, A. Hovnanian, J.A. Bouwstra, Intercellular skin barrier lipid composition and organization in Netherton syndrome patients, J. Investig. Dermatol. 134 (2014) 1238–1245.
[40] E.H. Mojumdar, R.W. Helder, G.S. Gooris, J.A. Bouwstra, Monounsaturated fatty acids reduce the barrier of stratum corneum lipid membranes by enhancing the formation of a hexagonal lateral packing, Langmuir 30 (2014) 6534–6543.
[41] B. Skolova, B. Janusova, J. Zbytovska, G. Gooris, J. Bouwstra, P. Slepicka, P. Berka, J. Roh, K. Palat, A. Hrabalek, K. Vavrova, Ceramides in the skin lipid membranes: length matters, Langmuir 29 (2013) 15624–15633.
[42] R. Mendelsohn, C.R. Flach, D.J. Moore, Determination of molecular conformation and permeation in skin via IR spectroscopy, microscopy, and imaging, Biochim. Biophys. Acta 1758 (2006) 923–933.
[43] A.Y. Alentiev, Y.P. Yampolskii, Free volume model and tradeoff relations of gas permeability and selectivity in glassy polymers, J. Membr. Sci. 165 (2000) 201–216.
[44] S.M. Fang, S.A. Stern, A "free volume" model of permeation of gas and liquid mixtures through polymeric membranes, Chem. Eng. Sci. 30 (1975) 773–780.
[45] L. Senak, M.A. Davies, R. Mendelsohn, A quantitative IR study of hydrocarbon chain conformation in alkanes and phospholipids: CH_2 wagging modes in disordered bilayer and HII phases, J. Phys. Chem. 95 (1991) 2565–2571.
[46] E.A. Disalvo, O.A. Pinto, M.F. Martini, A.M. Bouchet, A. Hollmann, M.A. Frias, Functional role of water in membranes updated: a tribute to Trauble, Biochim. Biophys. Acta 1848 (2015) 1552–1562.